

# Chip-scale Optical Resonator Enabled Synthesizer (CORES)

John E. Bowers<sup>1</sup>, Andreas Beling<sup>8</sup>, Steven M. Bowers<sup>8</sup>, Travis C. Briles<sup>8</sup>, Lin Chang<sup>1</sup>, Jeff Chiles<sup>6</sup>, Robert Costanzo<sup>8</sup>, Marcelo Davanco<sup>7</sup>, Scott A. Diddams<sup>6</sup>, Tara E. Drake<sup>6</sup>, Michael Geiselmann<sup>4</sup>, Bahareh Ghadiani<sup>3</sup>, B. Robert Ilic<sup>7</sup>, Akshar Jain<sup>1</sup>, David H. Kinghorn<sup>1</sup>, Tobias J. Kippenberg<sup>3</sup>, Qing Li<sup>7</sup>, Junqiu Liu<sup>3</sup>, Richard P. Mirin<sup>6</sup>, Gregory T. Moille<sup>7</sup>, Tiago Morais<sup>4</sup>, Jill L. Morton<sup>5</sup>, Paul A. Morton<sup>5</sup>, Nima Nader<sup>6</sup>, Scott B. Papp<sup>6</sup>, Nicolas Raduazo<sup>8</sup>, Arslan S. Raja<sup>3</sup>, Boqiang Shen<sup>2</sup>, Kartik A. Srinivasan<sup>7</sup>, Eric J. Stanton<sup>6</sup>, Jordan R. Stone<sup>6</sup>, Luke Theogarajan<sup>1</sup>, Minh A. Tran<sup>1</sup>, Kerry J. Vahala<sup>2</sup>, Nicolas Volet<sup>1</sup>, Rui Ning Wang<sup>3</sup>, Ye Wang<sup>8</sup>, Daron Westly<sup>7</sup>, Qifan Yang<sup>2</sup>, Zhanyu Yang<sup>8</sup>, Xu Yi<sup>8</sup>, Michael Zervas<sup>4</sup>

<sup>1</sup>UCSB ; <sup>2</sup>Caltech ; <sup>3</sup>EPFL ; <sup>4</sup>LiGenTec ; <sup>5</sup>Morton Photonics ; <sup>6</sup>NIST, Boulder ; <sup>7</sup>NIST, Gaithersburg ; <sup>8</sup>UVA

✉ [bowers@ece.ucsb.edu](mailto:bowers@ece.ucsb.edu)

**Abstract**— We describe research on an optical-frequency synthesizer in a low-power chip-scale package that provides a laser output with a programmable optical frequency across 50 nm of bandwidth centered at 1550 nm, with a resolution smaller than one part in  $10^{14}$ .

**Keywords**— heterogeneous integration; nonlinear optics; optical frequency combs; tunable lasers

## I. INTRODUCTION

Optical-frequency synthesizers, which generate light with stable frequency based on a single microwave-frequency reference, have proven extremely valuable in a variety of scientific endeavors, such as coherent light detection and ranging, atomic and molecular spectroscopy and optical communications. However, even though optical-frequency synthesizers based on mode locked lasers were demonstrated two decades ago, their use has been limited to laboratory settings due to the cost, size, and power requirements of their components.

Recently, the developments in heterogeneously integrated photonics and Kerr-soliton frequency combs generated by on-chip microresonators, have provided new solutions to address the aforementioned problems. By merging these technologies, we demonstrated a chip-scale optical-frequency synthesizer that can be programmed across 4 THz near 1550 nm with 1-Hz resolution and traceability to the SI second [1]. Mirroring the framework of traditional optical frequency synthesizers, Fig. 1 shows the schematic drawing of our system: the tunable laser is synthesized by phase-locking to a stabilized comb reference, using a look-up table (LUT) and a field-programmable gate array (FPGA). Here we give a description of the technologies involved in this project.

## II. 15-GHZ WAVEGUIDE COUPLED SOLITON SOURCE

Detectable pulse repetition rates are required in the reference frequency comb systems in order to interface the comb to electronics. To attain detectable pulse rates in a microcomb, it is necessary for the comb resonator diameter to be in the millimeter range so as to reduce the free-spectral-range (FSR). In the synthesizer work, this FSR (repetition rate) is set to 15 GHz,

corresponding to a 4.3-mm diameter. This specific rate is set to avoid Brillouin <sup>1</sup>effects that become important around 10 GHz.

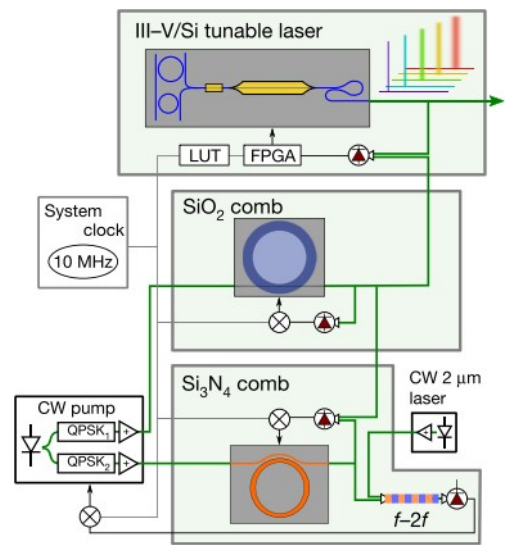


Fig. 1. Optical synthesizer composed of a heterogeneously integrated III-V/Si tunable laser, which is guided by dual dissipative-Kerr-soliton frequency combs fabricated on separate silicon chips and pumped by off-chip lasers[1].

Another challenge is to achieve a sufficiently high  $Q$  to overcome the large pump volume of the electronic-rate soliton comb. To avoid impractically-high pumping powers associated with the increased stored energy of these large diameter devices,  $Q$  factors well above those possible in existing integrable resonators are required. Furthermore, the design requirements imposed by soliton physics also include minimization of mode crossing and anomalous dispersion.

As part of this program, Caltech developed an ultra-high- $Q$  (UHQ) silica-on-silicon chip-based microresonator that combines unprecedented high- $Q$  performance with monolithic waveguide integration, by introducing a plasma-enhanced chemical vapor deposition (PECVD) silicon nitride waveguide. The micrograph image of this resonator is shown in Fig. 2(a).  $Q$  factors over 200 million are achieved in this integrated device

and a soliton microcomb having a detectable repetition rate is demonstrated at low operating powers [2], as shown in Fig. 2(b).

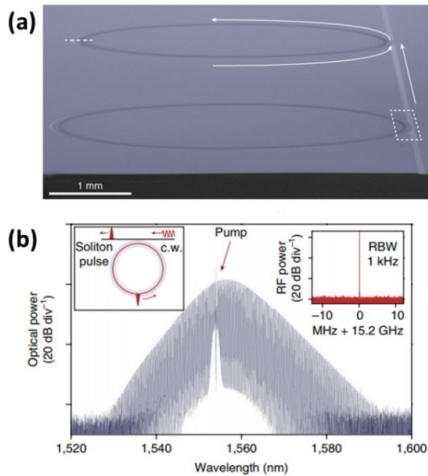


Fig. 2. (a) Micrograph image of the integrated ultrahigh-Q optical resonator; (b) Optical spectrum of soliton with pump line indicated. The left inset illustrates continuous-wave (c.w.) pumping to produce soliton mode locking of the resonator. The right inset shows the radio frequency (RF) power spectrum of the detected soliton pulse stream. RBW, resolution bandwidth [2].

### III. SILICON NITRIDE MICRO-RING RESONATORS

The self-referenced frequency comb technology relies on an octave-spanning soliton comb synchronized to the 15-GHz silica-based comb [3]–[5], which in this project is realized by a  $\text{Si}_3\text{N}_4$  planar waveguide coupled micro-ring resonator. The broadband frequency comb generation pumped in the telecom band requires  $\text{Si}_3\text{N}_4$  waveguides to have waveguide widths of 1.5–2  $\mu\text{m}$  and heights of 0.75–0.85  $\mu\text{m}$ . Furthermore, the waveguides should have low propagation loss to match semiconductor laser pump power capability. In this project NIST realized the required octave spanning resonators using subtractive fabrication of claddingless LPCVD  $\text{Si}_3\text{N}_4$ -based THz mode spacing resonators with. Careful dispersion engineering enabled octave spanning comb generation with dual dispersive waves, and simultaneous tuning of device parameters to achieve a carrier envelope frequency in the GHz range. This approach was used to realize the first integrated photonics based frequency synthesizer reported in Ref. [1].

In addition the program investigated ways to achieve lower loss optical integrated resonators. A new photonic Damascene process was developed to fabricate such low-loss and high-confinement waveguides. Instead of directly etching the highly stressed thick  $\text{Si}_3\text{N}_4$  film, the new process applied a dry etching onto a  $\text{SiO}_2$  layer, where the waveguide patterning was defined by deep ultraviolet (DUV) lithography. After the dry etch,  $\text{Si}_3\text{N}_4$  film is deposited on those pre-patterned recesses to form the waveguide structures. The dry etcher employed here allows several key etchant gases used in the process and more freedom to control the etch quality including uniformity, sidewall smoothness (passivation), and the sidewall angle. Meanwhile, a novel preform reflow step to further reduce the sidewall roughness was developed [6].

Another big advantage of the Damascene process is that it enables double nano-tapers which are widely used as chip input

couplers with high coupling efficiency and broad operation band. These waveguides are tapered both in width and height, and have enabled fiber-chip coupling with 1.5 dB/facet coupling loss [7].

Those advanced fabrication techniques lead to  $\text{Si}_3\text{N}_4$  microresonators with ultra-high intrinsic quality factor  $Q_0 > 15$  million, as shown in Fig. 3 (b) and (c) [8]. In these microresonators, soliton generation of 100 GHz repetition rate was successfully achieved with input power as low as 9.8 mW to the device. Such low power allows single soliton states to be accessed in multiple resonances without the use of an optical amplifier. Furthermore, octave spanning soliton combs have been obtained at pump wavelengths of both 1310 nm and 1550 nm [9], including dispersive wave generation. Fig. 3(d) and (e) shows the spectra of those combs.

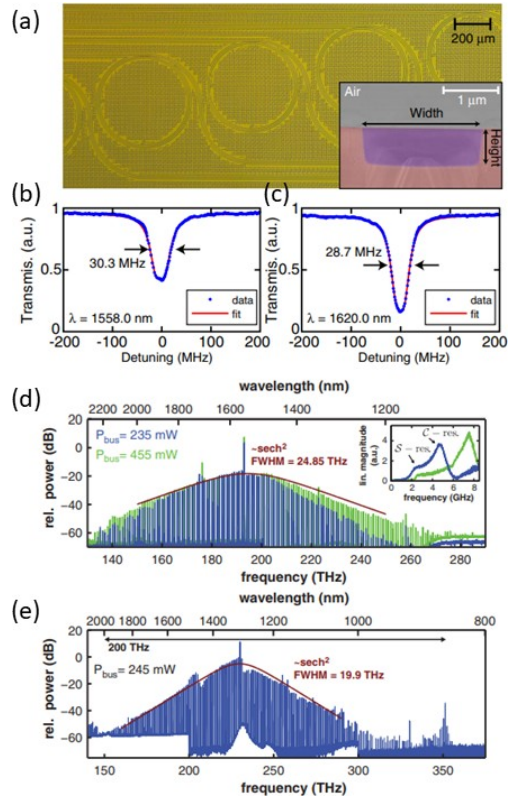


Fig. 3. (a) Microscope image of the  $\text{Si}_3\text{N}_4$  resonators. Inset: SEM image of the waveguide cross section; (b) and (c): Resonances and fits at different wavelengths; (d) and (e): Octave spanning soliton comb pumped around 1550 nm and 1310 nm, respectively [9].

### IV. SECOND HARMONIC GENERATION

One big challenge for the self-reference technology is to efficiently frequency double one tooth of the octave-spanning comb for offset frequency detection. After demonstrating the first periodically poled lithium niobate thin film waveguide for frequency conversion [10], recently we developed a new platform of Gallium Arsenide (GaAs) on insulator by heterogeneous integration for efficient second harmonic generation (SHG) [11]. Such a platform, owing to the high nonlinear coefficient of GaAs and strong index contrast of  $\text{SiO}_2$  confinement of GaAs waveguides, shows great potential for future nonlinear photonics.

The schematic drawing and SEM image of the waveguide cross section are shown in Fig. 4 (a) and (b), respectively. Fig. 4 (c) plots the experimental results of SHG for such a GaAs waveguide structure, pumped around 2000 nm wavelength. The normalized efficiency achieved here is one order of magnitude higher than other nonlinear platforms.

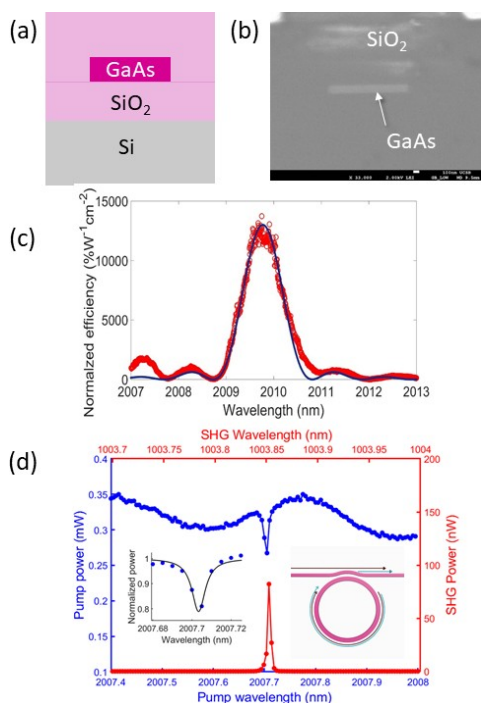


Fig. 4. (a) Schematic and (b) SEM of the cross section of GaAs on insulator waveguide (c) SHG experimental result of the waveguide; (d) Spectrum of the pump and SHG light for the GaAs resonator. The left inset is the experiment and fit for the pump resonance and the right inset is the structure of the ring resonator [11], [12].

A ring resonator based on such waveguide is also demonstrated [12] on this platform to further enhance the SHG, as illustrated in the inset of Fig. 4(d). According to the experimental results in Fig. 4(d), the quality factor of this resonator is higher than  $2.6 \times 10^5$ , and the external SHG efficiency is estimated to be  $\sim 100$  %/W. Depletion of pump power happens at very low power level, indicating extremely high internal conversion efficiency. Further optimization of the coupling will lead to much higher external efficiency and much more compact optical-frequency synthesizers. This extremely high conversion efficiency combined with the generation of double dispersive waves in the SiN comb spectrum [5] removes the need for an extra semiconductor optical amplifier at 2.0- $\mu\text{m}$  wavelength [13].

## V. LOW NOISE HIGH-POWER DIODE LASERS

Morton Photonics has reported an external-cavity diode laser (ECDL) with extremely narrow linewidth, low relative intensity noise, high output power, and useful spectral tunability [14, 15]. It emits 70 mW at 1550-nm wavelength, with a Lorentzian linewidth as narrow as 63 Hz. This spectral purity is orders of magnitude better than the current state-of-the-art ECDLs. As a preliminary application for this prototype, a temporal soliton is

directly generated and stabilized in a silica micro-resonator, without using an optical amplifier or a modulator [16], [17].

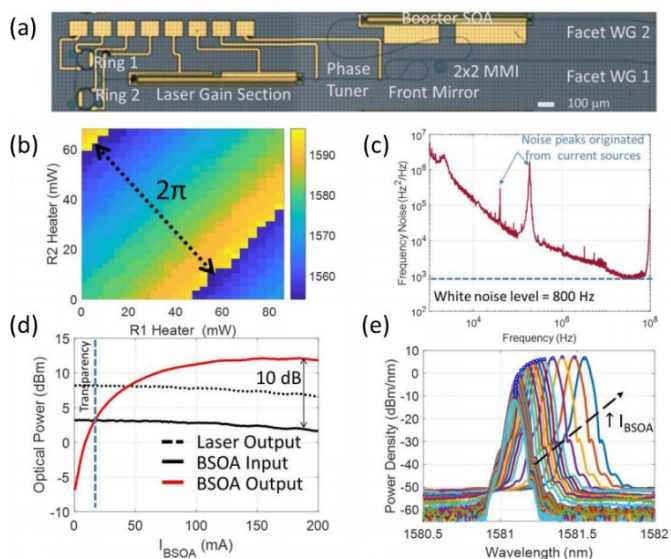


Fig. 5. (a) Microscopic photograph of the integrated laser with double ring mirror and a boosted SOA; (b) Wavelength tuning map as function of the power of the two rings; (c) Frequency noise spectrum; (d) Output power vs current injected to boosted SOA; (e) Optical spectra at the BSOA output with increasing injection levels. Blue circles are marked at the spectrum peaks to guide the eye [17].

Moving forward, an integrated version of such a laser has recently been demonstrated at UCSB on a III-V/Si heterogeneous platform [18]. Thanks to the greatly reduced propagation loss of silicon on insulator (SOI) waveguides and a novel multi-ring mirror design as the feedback, we successfully demonstrated a laser with 40 nm tuning range across the C+L band, a record-low 2.5 kHz Lorentzian linewidth, and output power up to 12 dBm. The laser structure and experimental results are shown in Fig. 5(a). This demonstration drastically reduces the complexity, size, and cost of the system, and is expected to enable a fully integrated source of solitons.

## VI. BALANCED PHOTORECEIVERS AND ELECTRONICS

To facilitate efficient and low-noise photodetection at GHz frequencies, balanced photoreceivers were developed at UVA with near-to-unity quantum efficiency along with low-noise transimpedance amplifiers (TIAs) [19]. The detector technology is now based on InP/InGaAs waveguide photodiodes that are heterogeneously integrated onto SiN waveguides on an interposer. The TIAs are designed to present low impedance to the photodiode, helping to maintain high bandwidths while amplifying the output RF signal to detectable levels. The early TIAs are fabricated in a 130-nm CMOS process, but more recent designs capable of achieving over 60 dB $\Omega$  gain across 10-GHz bandwidth, are fabricated in 65-nm and 55-nm processes.

An application specific integrated circuit (ASIC) has been fabricated using the Global Foundries 55-nm CMOS process to improve on the performance of the synthesis electronics previously demonstrated at the board level [20]. An on-chip broadband phase-locked loop (PLL, from DC to 8.25 GHz)

allows synthesis of optical heterodynes across that frequency range. In parallel, a new printed circuit board (PCB) has been designed with lower noise and higher speed current drivers. These upgrades pushed the synthesis bandwidth to 100 kHz for faster settling times and greater noise reduction. Locking the optical heterodyne between our tunable laser heterogeneously integrated on silicon and a reference laser, a frequency instability of  $2 \times 10^{-16}$  was achieved at 1-s averaging. This is a major improvement compared to our previous results [1], see Fig. 6. Our synthesizer now has a step resolution of 745 mHz and a mean deviation of 626  $\mu$ Hz from its setpoint, based on in-loop electronics controls of the tunable laser.

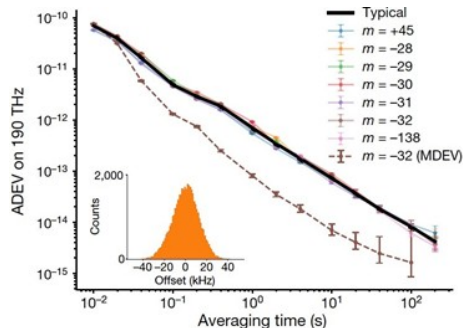


Fig. 6. Measured overlapping Allan deviation (ADEV) and modified Allan deviation (MDEV) of our frequency synthesizer [1]. The relative mode order of the silica comb is noted  $m$ .

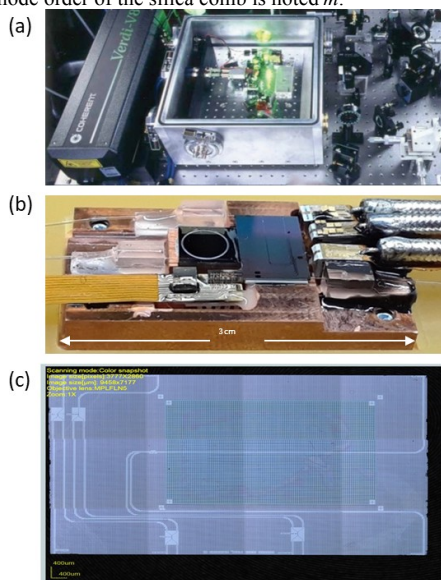


Fig. 7. Pictures of optical-frequency synthesizers: (a) Bench-top version ( $1.5 \text{ m}^3$ , 1 kW) based on a femtosecond laser comb; (b) Chip-scale DODOS version ( $1 \text{ cm}^3$ , 1 W) packaged during this work; (c) Microscopic image of the interposer chip.

## VII. INTERPOSER AND PACKAGING

One major goal of this work is to shrink all the discrete optical components thus far demonstrated into a small, manufacturable, and reliable module that can be mounted within common electronic assemblies. Compared to the previous bench-top version of the frequency synthesizer based on femtosecond laser comb [Fig. 7(a)], our recently demonstrated

package shown in Fig. 7(b) has  $> 1000$  times drop in size and power consumption, and  $> 100$  times decrease in terms of cost.

This architecture uses a  $\text{Si}_3\text{N}_4$  interposer chip to combine and mix the signals originating from the two frequency comb chips ( $\text{Si}_3\text{N}_4$  octave-spanning, THz mode spacing comb and silica C-band-spanning, 15-GHz mode spacing comb) and the output tunable laser, from Fig. 7(c). This interposer chip also contains a heterogeneously-integrated GaAs region to perform the critical second harmonic generation step for  $f$ - $2f$  self-referencing of the octave-spanning comb. Our new interposer architecture also incorporates waveguide photodetectors for measuring the three different beat note signals ( $f_0$ ,  $\text{Si}_3\text{N}_4$  comb/silica comb, and silica comb/tunable laser), which represents a significant reduction in the size of the overall assembly. This also requires the incorporation of on-chip filtering and polarization rotation that were handled off-chip in previous work [1].

## REFERENCES

- [1] D. T. Spencer *et al.*, “An optical-frequency synthesizer using integrated photonics,” *Nature* **557**, 81–85, 2018.
- [2] K. Y. Yang *et al.*, “Bridging ultrahigh-Q devices and photonic circuits,” *Nat. Photonics* **12**, 297–302, 2018.
- [3] T. C. Briles *et al.*, “Interlocking Kerr-microresonator frequency combs for microwave to opt. synthesis,” *Opt. Lett.* **43**, 2933, 2018.
- [4] J. R. Stone *et al.*, “Thermal and Nonlinear Dissipative-Soliton Dynamics in Kerr-Microresonator Frequency Combs,” *Phys. Rev. Lett.* **121**, 063902, 2018.
- [5] Q. Li *et al.*, “Stably accessing octave-spanning microresonator frequency combs in the soliton regime,” *Optica*, vol. 4, p. 193, 2017.
- [6] M. H. P. Pfeiffer, *et al.*, “Ultra-smooth silicon nitride waveguides based on the Damascene reflow process: fabrication and loss origins,” *Optica* **5**, 884, 2018.
- [7] J. Liu *et al.*, “Double inverse nanotapers for efficient light coupling to integrated photonic devices,” *Opt. Lett.* **43**, 3200, 2018.
- [8] J. Liu *et al.*, “Ultralow-power chip-based soliton microcombs for photonic integration,” *Optica* **5**, 1347, 2018.
- [9] M. H. P. Pfeiffer *et al.*, “Octave-spanning dissipative Kerr soliton frequency combs in  $\text{Si}_3\text{N}_4$  microresonators,” *Optica*, **4**, p. 684, 2017.
- [10] L. Chang, Y. Li, N. Volet, L. Wang, J. Peters, and J. E. Bowers, “Thin film wavelength converters for photonic integrated circuits,” *Optica* **3**, 531, 2016.
- [11] L. Chang *et al.*, “Heterogeneously integrated GaAs waveguides on insulator for efficient freq. conversion,” *Laser Photon. Rev.*, 2018.
- [12] L. Chang *et al.*, “Strong frequency conversion in heterogeneously integrated GaAs resonators,” *IPC postdeadline*, 2018.
- [13] N. Volet *et al.*, “Semiconductor optical amplifiers at 2.0- $\mu\text{m}$  wavelength on silicon,” *Laser Photon. Rev.* **11**, 1600165, 2017.
- [14] P. Morton *et al.*, “High-power, ultra-low noise hybrid lasers for microwave photonics and optical sensing,” *JLT*, **36**, 5048, 2018.
- [15] N. Volet *et al.*, “Micro-resonator soliton generated directly with a diode laser,” *Laser Photon. Rev.* **12**, 1700307, 2018.
- [16] X. Yi, *et al.*, “Active capture and stabilization of temporal solitons in microresonators,” *Opt. Lett.* **41**, 2037, 2016.
- [17] V. Brasch, *et al.* “Bringing short-lived dissipative Kerr soliton states in microresonators into steady state,” *Opt. Express* **24**, 29312, 2016.
- [18] M. A. Tran, *et al.*, “A 2.5 kHz linewidth widely tunable laser with booster SOA integrated on silicon,” in *ISLC*, 2018, pp. 1–2.
- [19] R. Costanzo, *et al.*, “A 10-GHz bandwidth balanced photoreceiver with 41 V/W optical conversion gain,” in *EuMIC*, 2017, p. 154.
- [20] A. Bluestone *et al.*, “Heterodyne-based hybrid controller for wide dynamic range OE freq. synthesis,” *Opt. Express* **25**, 29086, 2017.